



Cite this: RSC Adv., 2015, 5, 70522

Received 22nd June 2015  
 Accepted 11th August 2015  
 DOI: 10.1039/c5ra12002k  
[www.rsc.org/advances](http://www.rsc.org/advances)

## Introduction

Graphene, a one atom thick sheet of  $sp^2$  carbon atoms arranged in a honeycomb configuration, has been intensively studied as a novel 2D material in recent years. Its prominent mechanical, electronic and chemical properties make graphene a key material for next-generation technologies.<sup>1,2</sup> Doping graphene with heteroatoms is one of the most promising methods for modifying its properties.<sup>3</sup> It is reported that nitrogen (N) doping gives rise to the evolution of a band gap.<sup>4,5</sup> Opening the band gap leads to a high on/off ratio, which is essential for application to electronic devices. Another interesting phenomenon evoked by N-doping is the catalytic activity for oxygen reduction reaction,<sup>6</sup> the cathode reaction of fuel cells. Carbon alloy catalysts (CACs), the assembly of N-doped graphene, can be seen as an inexpensive alternative to platinum.<sup>7,8</sup> With regard to CACs, increased conductivity by electron doping as a result of N-doping is important rather than emergence of a band gap. Despite the many studies on the synthesis of N-doped graphene,<sup>9–17</sup> controlling the doping level is still a big challenge. One of the major reasons is the trade-off relationship between the degree of graphenization and the N-doping amount; the former requires a high growth temperature, while the latter decreases rapidly with temperature.<sup>13–17</sup> To overcome such a dilemma, a N-doping method effective still at room temperature is required. In addition, a direct N-doping method to graphene

The effect of nitrogen doping on graphene was characterized without exposing the prepared specimen to the atmosphere. Nitrogen doping was done via a photochemical process at room temperature, in which graphene on  $SiO_2/Si$  was irradiated by UV light in ammonia. Field effect transistor measurements revealed that the UV-irradiation of graphene in  $NH_3$  causes electron doping of  $\sim 10^{12} \text{ cm}^{-2}$  ( $\sim 0.01\%$ ) as a result of N-doping, which can be controlled by changing the irradiation time. Comparing the transfer characteristics and the Raman spectra, we discuss the structure of the graphene functionalized via photochemical reactions, and the corresponding electronic structure.

that can control the doping level has been highly anticipated. Most of past studies using chemical vapour deposition (CVD) needed a transfer process for characterization, which made it difficult to deduce the intrinsic nature of doping due to the inevitable subsidiary effect.

In our previous study, we succeeded in fabricating N-doped graphene by exposing the graphene to  $NH_3$  atmosphere under UV light irradiation.<sup>18</sup> This method enables us to characterize the electrical properties before and after N-doping *in situ*. In the present study, we have observed a shift of the charge neutrality point (CNP) to the negative direction after the UV-irradiation in  $NH_3$ , which indicates electron doping to graphene. The doping levels can be controlled in the range of  $10^{12}$  to  $10^{13} \text{ cm}^{-2}$  by varying the irradiation time. On the basis of transport measurements and Raman spectroscopy, we discuss the possible structure for the N-doped graphene.

## Experimental

There are several methods to fabricate graphene such as mechanical exfoliation of graphite, epitaxial growth on SiC, reduction of graphene oxide, and CVD process including solid carbon sources.<sup>19–25</sup> To ensure the quality and uniformity of graphene on  $SiO_2$ , we purchased graphenes on  $SiO_2$  (285 nm)/Si from Graphene Laboratories Inc., which were fabricated via CVD process. The specimens were taken from the same lot. Fig. 1 shows a schematic illustration of the experimental setup. To fabricate a field effect transistor (FET) structure, 20 nm-thick gold pads were deposited onto the graphene as source and drain electrodes. After wiring the electrodes to vacuum feed-throughs, the chamber was evacuated to  $\sim 10^{-6} \text{ Pa}$ . Electrical measurements and UV-irradiation were performed in the vacuum chamber. Prior to electrical measurements, the graphene was annealed in a vacuum at 160 °C for several hours, which removed adsorbed molecules and contaminants.

<sup>a</sup>World Premier International (WPI) Research Center, International Center for Materials Nanoarchitectonics (MANA), National Institute for Materials Science (NIMS), 1-1 Namiki, Tsukuba, Ibaraki 305-0044, Japan. E-mail: IMAMURA.Gaku@nims.go.jp; Fax: +81-29-860-4706; Tel: +81-29-851-3354 ext. 4186

<sup>b</sup>Department of Complexity Science and Engineering, Graduate School of Frontier Sciences, The University of Tokyo, Kashiwanoha 5-1-5, Kashiwa, Chiba 277-8561, Japan

† Electronic supplementary information (ESI) available. See DOI: 10.1039/c5ra12002k



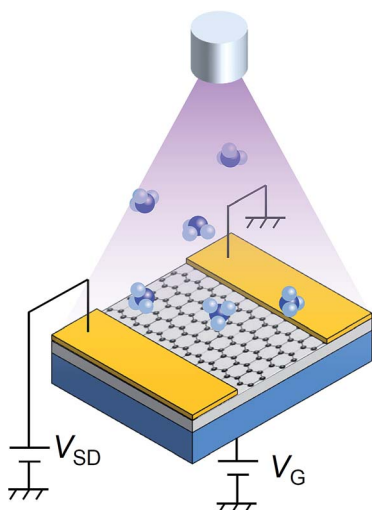


Fig. 1 Schematic illustration of the experimental setup.

Ammonia was introduced into the chamber *via* a variable leak valve. A deuterium lamp (L2D2, 30 W, Hamamatsu Photonics K.K.) was used for UV-irradiation. The peak emission wavelength of the lamp is around 150–200 nm, and the effective power density is estimated to  $\sim 0.01$  mW cm $^{-2}$ . Raman spectroscopy was performed in air with excitation wavelength of 532 nm.

## Results and discussion

Fig. 2a shows the FET characteristics of the graphene before and after UV-irradiation in NH<sub>3</sub>. Typical transfer characteristics of pristine graphene could be observed before the UV-irradiation,<sup>26</sup> CNP was located at around 0 V, and the curve exhibited a small hysteresis. The carrier mobility of the graphene was  $1100$  cm $^2$  (V $^{-1}$  s $^{-1}$ ) and  $2300$  cm $^2$  (V $^{-1}$  s $^{-1}$ ) for electron and hole transport, respectively. After the FET measurement, the graphene was UV-irradiated under 10 Pa of NH<sub>3</sub> for 1 h at RT. The evolution of a hysteresis and the decrease of mobility was observed after the UV-irradiation (Fig. 2a). For the forward sweep (from a negative to a positive gate voltage), the electron mobility ( $\mu_e$ ) and hole mobility ( $\mu_h$ ) decreased to  $720$  cm $^2$  (V $^{-1}$  s $^{-1}$ ) and  $1200$  cm $^2$  (V $^{-1}$  s $^{-1}$ ), respectively.  $\mu_e$  and  $\mu_h$  for the backward sweep (from a positive to a negative gate voltage) were  $790$  cm $^2$  (V $^{-1}$  s $^{-1}$ ) and  $940$  cm $^2$  (V $^{-1}$  s $^{-1}$ ), respectively. The evolution of a hysteresis and the decrease of mobility were explained by the formation of sp<sup>3</sup>-like bonds at the graphene/SiO<sub>2</sub> interface as described in ref. 27. Our previous study showed that UV-irradiation in a vacuum triggers a photochemical reaction at the graphene/SiO<sub>2</sub> interface, which gives rise to the decrease in mobility and the hysteresis that was counter clockwise on the negative side and clockwise on the positive side. Another noticeable change in FET characteristics after the UV-irradiation in NH<sub>3</sub> was a shift in the CNP to the negative direction. The CNP is shifted by  $-16$  V after the UV-irradiation in NH<sub>3</sub>, while UV-irradiation in a vacuum does not shift the CNP.<sup>27</sup> Hence, it is implied that the CNP is shifted to the negative direction as a result of N-doping, by which

nitrogen atoms are incorporated into the graphene lattice. Incorporation of N atoms by UV irradiation in ammonia was confirmed by X-ray photoelectron spectroscopy in our previous study.<sup>18</sup>

Fig. 2b shows the Raman spectra of the graphene before and after the UV-irradiation in NH<sub>3</sub>. Three inherent peaks for graphene are seen for both spectra: the G band ( $\sim 1585$  cm $^{-1}$ ), the D band ( $\sim 1350$  cm $^{-1}$ ), and the 2D band ( $\sim 2700$  cm $^{-1}$ ).<sup>28</sup> The D band originating from the A<sub>1g</sub> vibrational mode of hexagonal sp<sup>2</sup> carbon network becomes Raman active by defects. Therefore, the intensity ratio of the D band to the G band ( $I_D/I_G$ ) is a good indicator for evaluating the density of defects.<sup>29,30</sup> While the pristine graphene showed small  $I_D/I_G$  ( $0.11 \pm 0.05$ ), the graphene UV-irradiated in NH<sub>3</sub> exhibited higher  $I_D/I_G$  ( $0.22 \pm 0.08$ ). Thus defects were introduced into the graphene lattice by the UV-irradiation in NH<sub>3</sub>. As the sharp symmetric 2D band was not substantially changed after irradiation, the structure of monolayer graphene remained.<sup>31</sup> The widening of the 2D band reflects the defect formation in graphene.<sup>32,33</sup>

To investigate the dependence on the irradiation time, graphene was UV-irradiated in 10 Pa of NH<sub>3</sub> for longer times (2 h and 4 h). The shift in CNP ( $\Delta V_{CNP}$ ) was plotted as a function of

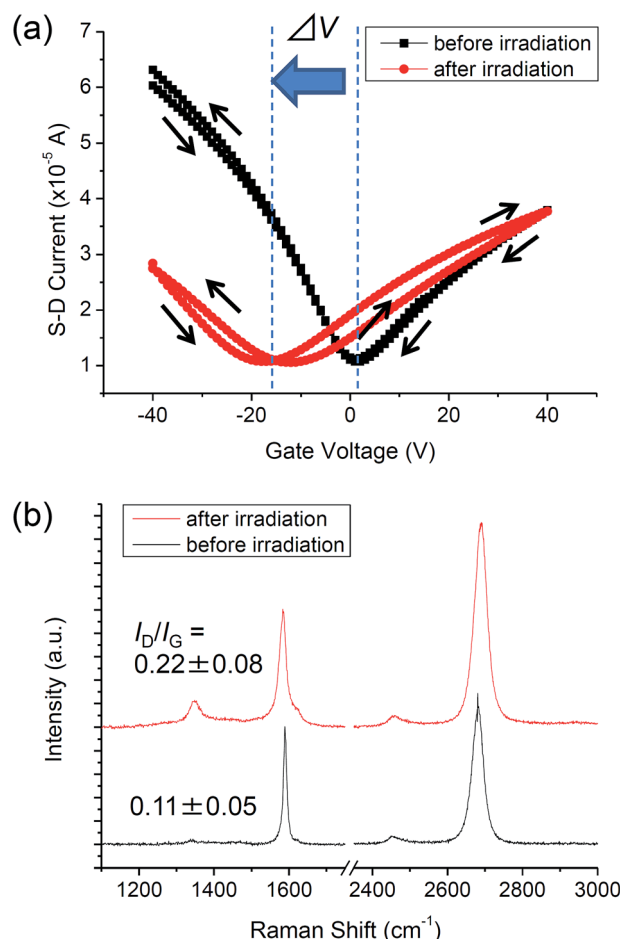


Fig. 2 (a) Transfer characteristics of graphene before and after the UV-irradiation in NH<sub>3</sub>. (b) Raman spectra of graphene before and after the UV-irradiation in NH<sub>3</sub>.



irradiation time in Fig. 3a.  $\Delta V_{\text{CNP}}$  is almost proportional to the irradiation time. We estimate the doped electron density ( $n_e$ ) from  $\Delta V_{\text{CNP}}$  according to the capacitor relationship:  $n_e = C_{\text{ox}}\Delta V_{\text{CNP}}/e$ , where  $C_{\text{ox}}$  and  $e$  are the capacitance of  $\text{SiO}_2$  per area and the elementary charge, respectively.  $n_e$  for the graphene UV-irradiated in  $\text{NH}_3$  for 1 h, 2 h, and 4 h is estimated to  $1.3 \times 10^{12} \text{ cm}^{-2}$ ,  $3.4 \times 10^{12} \text{ cm}^{-2}$ ,  $6.1 \times 10^{12} \text{ cm}^{-2}$ , respectively. Considered that the atomic number density of graphene is  $3.8 \times 10^{15} \text{ cm}^{-2}$ , the corresponding doping level for the graphene UV-irradiated in  $\text{NH}_3$  for 1 h, 2 h, and 4 h is 0.034%, 0.089%, and 0.16%, respectively. Thus the electron density of graphene can be controlled in the range of  $10^{12}$  to  $10^{13} \text{ cm}^{-2}$  (0.01%) by the UV-irradiation in  $\text{NH}_3$ . With regard to carrier mobility, the changes in electron and hole mobility ( $\mu_e$  and  $\mu_h$ , respectively) are summarised in Table 1.

To elucidate the relation between the N-doping and the formation of  $\text{sp}^3$ -like bonds by the UV-irradiation, we compared the results with the data from the graphene UV-irradiated in a vacuum.<sup>27</sup> With regard to the FET characteristics, the CNP is shifted to the negative side after UV-irradiation in  $\text{NH}_3$ , while the CNP stays at around 0 V for the graphene UV-irradiated in a vacuum (Fig. 3a). The difference between  $\text{NH}_3$  and vacuum can

Table 1 Mobility and charge neutrality point for each sample

	Irradiation time	$\mu_e (\text{cm}^2 \text{ V}^{-1} \text{ s}^{-1})$	$\mu_h (\text{cm}^2 \text{ V}^{-1} \text{ s}^{-1})$	$V_{\text{CNP}} (\text{V})$
1 h	Before	1000	2300	1
	After ( $- \rightarrow +$ )	720	1200	-18
	After ( $+ \rightarrow -$ )	790	940	-12
2 h	Before	1500	1800	2
	After ( $- \rightarrow +$ )	710	790	-41
	After ( $+ \rightarrow -$ )	770	640	-38
4 h	Before	1200	1600	3
	After ( $- \rightarrow +$ )	510	— <sup>a</sup>	-73
	After ( $+ \rightarrow -$ )	500	— <sup>a</sup>	-70

<sup>a</sup> Mobility cannot be calculated because gate voltage more negative than 80 V could not be applied to prevent dielectric breakdown.

also be seen in the change of Raman spectra as shown in Fig. 3b. While the  $I_D/I_G$  monotonically increased with irradiation time for both conditions, the degree of increase is larger for the UV-irradiation in  $\text{NH}_3$  than that in a vacuum. This higher  $I_D/I_G$  implies that graphene is damaged by N-doping as well as the formation of  $\text{sp}^3$ -like bonds caused by UV-light.

The effect of adsorption of ammonia on graphene was also studied by exposing the graphene on  $\text{SiO}_2/\text{Si}$  to 10 Pa of  $\text{NH}_3$  for 1 h without UV-light. Fig. 4a shows the FET characteristics before and after the exposure. No noticeable change can be observed after the UV-irradiation without a small shift of CNP to the negative direction. Such small negative shift after the exposure to  $\text{NH}_3$  has also been reported by Romero *et al.*, which is considered to be caused by displacement chemical reactions in the graphene/ $\text{SiO}_2$  interface.<sup>34</sup> The Raman spectra also showed no changes at all (Fig. 4b).

On the basis of the experimental results, we propose a possible structure of N-doped graphene together with the electronic structure in Fig. 5. Before the UV-irradiation in  $\text{NH}_3$ , the Fermi level was located at the Dirac point judging from the  $V_{\text{CNP}}$  of around 0 V (Fig. 2a). The shift of the CNP after the UV-irradiation in  $\text{NH}_3$  indicated that electrons were doped into graphene, and the Fermi level was shifted to higher energy. It is known that UV light induces a photodissociation reaction of  $\text{NH}_3$  molecules described as



which yields active  $\text{NH}_2$  radicals.<sup>35</sup> As the activation energy for this reaction is 6.0 eV (corresponding to photon with a wavelength of 206 nm), the deuterium lamp used in this study can induce this reaction. By means of chemical reactions between such  $\text{NH}_2$  radicals and graphene, we have reported that graphene is functionalized with amino groups as well as the formation of  $\text{g-C}_3\text{N}_4$  domains.<sup>18</sup> Several studies have reported that amino groups would act as an electron donor for graphene,<sup>36,37</sup> hence the amino groups introduced *via* the photochemical reaction are responsible for the electron doping. In addition to the amino groups and  $\text{g-C}_3\text{N}_4$  domains,  $\text{sp}^3$ -like bonds are also formed at the graphene/ $\text{SiO}_2$  interface,<sup>18,27</sup> which are responsible for the decrease in the carrier mobility and the

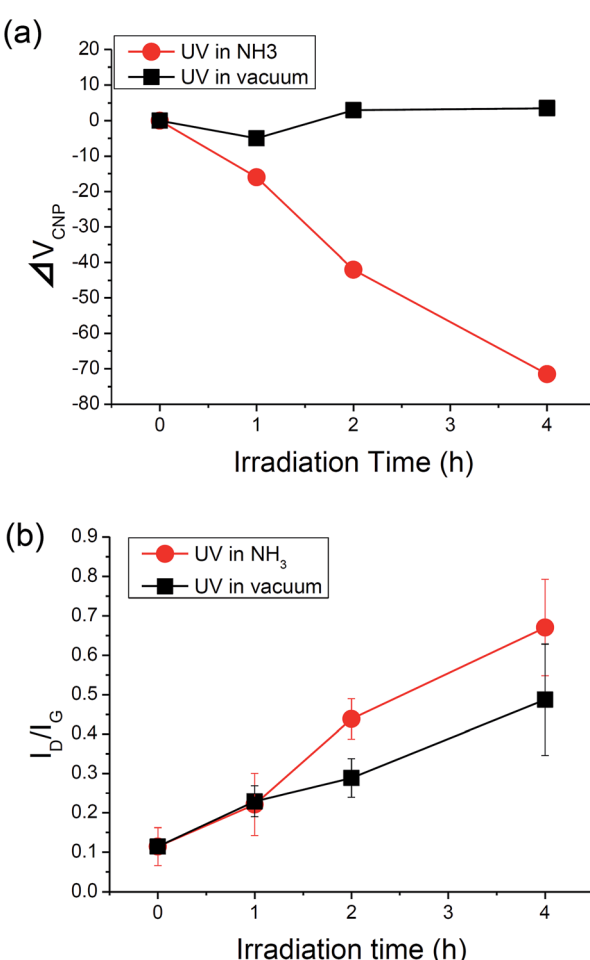


Fig. 3 (a)  $\Delta V_{\text{CNP}}$  as a function of irradiation time. (b) Raman  $I_D/I_G$  as a function of irradiation time.

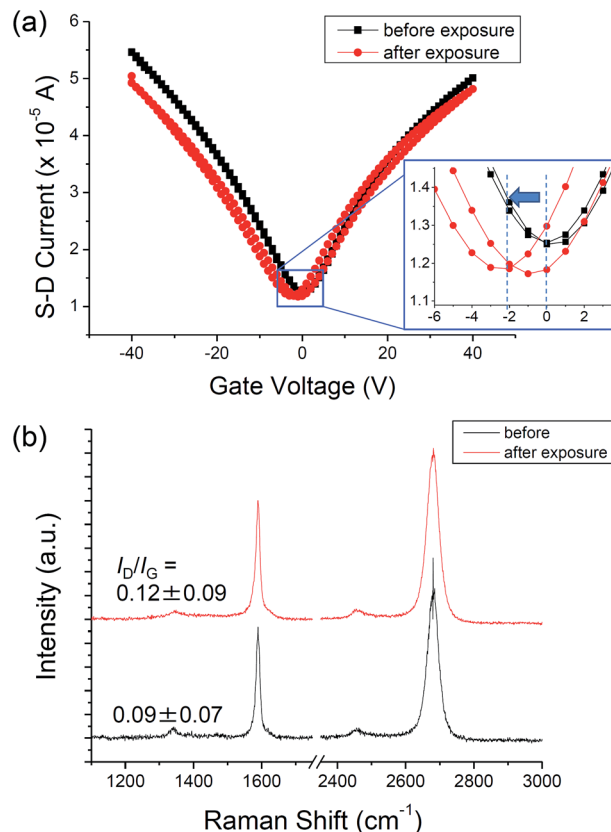


Fig. 4 (a) Transfer characteristics of graphene before and after exposure to  $\text{NH}_3$ . (Inset) Enlarged transfer characteristics at around the Dirac point. (b) Raman spectra of graphene before and after exposure to  $\text{NH}_3$ .

hysteresis behaviour. Such undesirable defects may be reduced by indirect UV irradiation in ammonia, by which the graphene sample is not directly UV-irradiated.

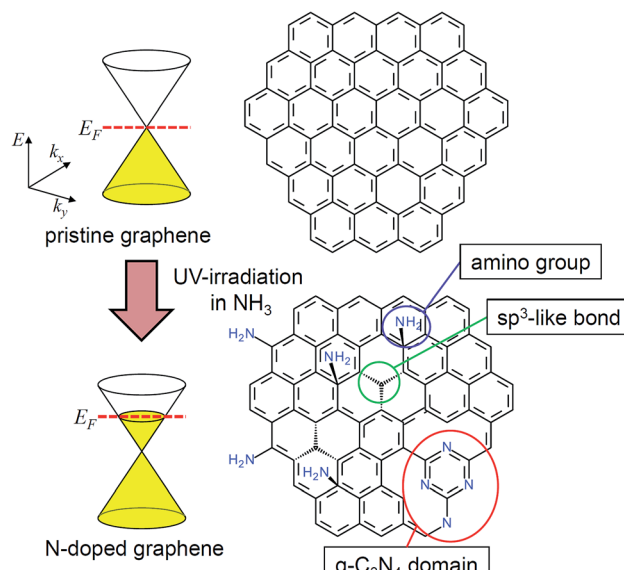


Fig. 5 Schematic illustration of N-doped graphene and the corresponding electronic structure.

The density of defects ( $\sigma_d$ ) can be estimated from the Raman  $I_D/I_G$ . According to the Tuinstra–Koenig relation, the average crystalline size ( $L_a$ ) is described as  $L_a = C/(I_D/I_G)$ , where  $C$  is a constant depending on the excitation wavelength ( $C = 19.2$  for 532 nm).<sup>29,30,38</sup> As  $L_a$  is the average distance between the defects,  $\sigma_d$  is written as  $\sigma_d = 1/L_a^2 = (I_D/I_G)^2/C^2$ . Note that any structural disorders including vacancies, sp<sup>3</sup> carbon structures, and doped impurities contribute to  $\sigma_d$  in this estimation. As  $I_D/I_G$  was  $0.22 \pm 0.08$  for the graphene UV-irradiated in  $\text{NH}_3$  for 1 h,  $\sigma_d$  is estimated to be  $1.26 \times 10^{10} \text{ cm}^{-2}$ , which is approximately 1/100 of the doped electron density ( $n_e$ ) estimated from the shift of the CNP ( $1.3 \times 10^{12} \text{ cm}^{-2}$ ). This significant deviation implies that defect formation including N-doping occurs rather locally. The estimation of  $\sigma_d$  assumes randomly distributed defects in graphene. Therefore  $\sigma_d$  is likely to be underestimated if defects are locally formed. It is highly plausible that defects are localized in some regions of graphene. Formation of g-C<sub>3</sub>N<sub>4</sub> domains is one of such examples. As we have discussed in the previous study, X-ray photoelectron spectroscopy implies that g-C<sub>3</sub>N<sub>4</sub> domains are formed in the graphene lattice.<sup>18</sup> Another case is that defects such as amino groups or sp<sup>3</sup>-like bond are localized at the periphery of graphene grains. As it is known that graphene is more reactive at grain boundaries than at a centre of domains,<sup>39–41</sup> defect formation is likely to occur at the periphery of domains.

Another explanation for the smaller defect density is the fact that defect density can be underestimated for the UV-induced defects. The studies on estimation of  $L_a$  or  $\sigma_d$  from the Raman  $I_D/I_G$  are based on the physically induced defects caused by ion-bombardment. However,  $I_D/I_G$  should depend on the types of defects.<sup>42</sup> On the basis of the phenomenological model,<sup>30</sup> we conclude that both sp<sup>3</sup>-like bonds and amino groups give rise to lower  $I_D/I_G$  than the structural disorders caused by ion-bombardment, resulting in the smaller defect density. The details are provided in the ESI.†

## Conclusions

Graphene on a  $\text{SiO}_2/\text{Si}$  substrate was irradiated by UV-light in  $\text{NH}_3$  at room temperature, and its FET characteristics were measured before and after the irradiation *in situ*. The electrical measurement has revealed that the electrons are doped *via* N-doping. By means of UV-irradiation in  $\text{NH}_3$ , we have demonstrated that electron doping level can be controlled in the range of  $10^{12}$  to  $10^{13} \text{ cm}^{-2}$  (0.01%). The FET measurements and the Raman spectroscopy indicate that N atoms are doped as amino groups and g-C<sub>3</sub>N<sub>4</sub> domains, and defects including N-containing species are formed rather locally. This study shows a possibility of N-doping *via* UV-irradiation, and provide a new strategy to modify the electronic properties of graphene.

## Acknowledgements

This work was supported by the New Energy and Industrial Technology Development Organization (NEDO) and also by a Grant-in-Aid for Scientific Research from MEXT of Japan (No. 25107002).



## Notes and references

1 K. S. Novoselov, V. I. Faíko, L. Colombo, P. R. Gellert, M. G. Schwab and K. Kim, *Nature*, 2012, **490**, 192–200.

2 H. Choi, S. Jung, J. Seo, D. W. Chang, L. Dai and J. Baek, *Nano Energy*, 2012, **1**, 534–551.

3 H. Liu, Y. Liu and D. Zhu, *J. Mater. Chem.*, 2011, **21**, 3335–3345.

4 A. Lherbier, A. Rafael, B. Méndez and J. C. Charlier, *Nano Lett.*, 2013, **13**, 1446–1450.

5 D. Usachov, O. Vilkov, A. Grüneis, D. Haberer, A. Fedorov, V. K. Adamchuk, A. B. Preobrajenski, P. Dudin, A. Barinov, M. Oehzelt, C. Laubschat and D. V. Vyalikh, *Nano Lett.*, 2011, **11**, 5401–5407.

6 Z. Yang, H. Nie, X. Chen, X. Chen and S. Huang, *J. Power Sources*, 2013, **236**, 238–249.

7 T. Ikeda, M. Boero, S. Huang, K. Terakura, M. Oshima and J. Ozaki, *J. Phys. Chem. C*, 2008, **112**, 14706–14709.

8 G. Chai, Z. Hou, D. Shu, T. Ikeda and K. Terakura, *J. Am. Chem. Soc.*, 2014, **136**, 13629–13640.

9 X. Wang, X. Li, L. Zhang, Y. Yoon, P. K. Weber, H. Wang, J. Guo and H. Dai, *Science*, 2009, **324**, 768–771.

10 D. Wei, Y. Liu, Y. Wang, H. Zhang, L. Huang and G. Yu, *Nano Lett.*, 2009, **9**, 1752–1758.

11 D. Long, W. Li, L. Ling, J. Miyawaki, I. Mochida and S. Yoon, *Langmuir*, 2010, **26**, 16096–16102.

12 C. Zhang, L. Fu, N. Liu, M. Liu, Y. Wang and Z. Liu, *Adv. Mater.*, 2011, **23**, 1020–1024.

13 G. Imamura and K. Saiki, *J. Phys. Chem. C*, 2011, **115**, 10000–10005.

14 G. Imamura, C. Chang, Y. Nabae, M. Kakimoto, S. Miyata and K. Saiki, *J. Phys. Chem. C*, 2012, **116**, 16305–16310.

15 T. Katoh, G. Imamura, S. Obata, M. Bhanuchandra, G. Copley, H. Yorimitsu and K. Saiki, *Phys. Chem. Chem. Phys.*, 2015, **17**, 14115–14121.

16 T. Terasawa and K. Saiki, *Jpn. J. Appl. Phys.*, 2012, **51**, 055101.

17 T. Katoh, G. Imamura, S. Obata and K. Saiki, *Carbon*, 2015, submitted.

18 G. Imamura and K. Saiki, *Chem. Phys. Lett.*, 2013, **587**, 56–60.

19 M. Cai, D. Thorpe, D. H. Adamson and H. C. Schniepp, *J. Mater. Chem.*, 2012, **22**, 24992–25002.

20 W. Norimatsu and M. Kusunoki, *Phys. Chem. Chem. Phys.*, 2014, **16**, 3501–3511.

21 F. Perrozzi, S. Prezioso and L. Ottaviano, *J. Phys.: Condens. Matter*, 2015, **27**, 013002.

22 Y. Zhang, L. Zhang and C. Zhou, *Acc. Chem. Res.*, 2013, **46**, 2329–2339.

23 Z. Sun, Z. Yan, J. Yao, E. Beitler, Y. Zhu and J. M. Tour, *Nature*, 2010, **468**, 549–552.

24 A. K. Kesarwani, O. S. Panwar, S. Chockalingam, A. Bisht, S. R. Dhakate, B. P. Singh, A. K. Srivastava and R. K. Rakshit, *Sci. Adv. Mater.*, 2014, **6**, 2124–2133.

25 O. S. Panwar, A. K. Kesarwani, S. R. Dhakate, B. P. Singh, R. K. Rakshit, A. Bisht and S. Chockalingam, *J. Vac. Sci. Technol., B: Microelectron. Nanometer Struct.–Process., Meas., Phenom.*, 2013, **31**, 040602.

26 F. Schwierz, *Nat. Nanotechnol.*, 2010, **5**, 487–496.

27 G. Imamura and K. Saiki, *ACS Appl. Mater. Interfaces*, 2015, **7**, 2439–2443.

28 L. M. Malard, M. A. Pimenta, G. Dresselhaus and M. S. Dresselhaus, *Phys. Rep.*, 2009, **473**, 51–87.

29 A. C. Ferrari and J. Robertson, *Phys. Rev. B: Condens. Matter Mater. Phys.*, 2000, **61**, 14095.

30 M. M. Lucchese, F. Stavale, E. H. M. Ferreira, C. Vilani, M. V. O. Moutinho, R. B. Capaz, C. A. Achete and A. Jorio, *Carbon*, 2010, **48**, 1592–1597.

31 A. C. Ferrari, J. C. Meyer, V. Scardaci, C. Casiraghi, M. Lazzeri, F. Mauri, S. Piscanec, D. Jiang, K. S. Novoselov, S. Roth and A. K. Geim, *Phys. Rev. Lett.*, 2006, **97**, 187401.

32 D. C. Kim, D.-Y. Jeon, H.-J. Chung, Y. S. Woo, J. K. Shin and S. Seo, *Nanotechnology*, 2009, **20**, 375703.

33 L. Liu, S. Ryu, M. R. Tomasik, E. Stolyarova, N. Jung, M. S. Hybertsen, M. L. Steigerwald, L. E. Brus and G. W. Flynn, *Nano Lett.*, 2008, **8**, 1965–1970.

34 H. E. Romero, P. Joshi, A. K. Gupta, H. R. Gutierrez, M. W. Cole, S. A. Tadigadapa and P. C. Eklund, *Nanotechnology*, 2009, **20**, 245501.

35 J. Biesner, L. Schnieder, G. Ahlers, X. Xie and K. H. Welge, *J. Chem. Phys.*, 1989, **91**, 2901–2911.

36 F. Liu, N. Tang, T. Tang, Y. Liu, Q. Feng, W. Zhong and Y. Du, *Appl. Phys. Lett.*, 2015, **106**, 013110.

37 I. Lee, H. Park, J. Park, J. Lee, W. Jung, H. Yu, S. Kim, G. Kim and J. Park, *Org. Electron.*, 2013, **14**, 1586–1590.

38 F. Tuinstra and J. L. Koenig, *J. Chem. Phys.*, 1970, **53**, 1126–1130.

39 D. Jiang, B. G. Sumpter and S. Dai, *J. Chem. Phys.*, 2007, **126**, 134701.

40 R. Sharma, J. H. Baik, C. J. Perera and M. S. Strano, *Nano Lett.*, 2010, **10**, 398–405.

41 N. Mitoma and R. Nouchi, *Appl. Phys. Lett.*, 2013, **103**, 201605.

42 S. Niyogi, E. Belyarova, M. E. Itkis, H. Zhang, K. Sheppard, J. Hicks, M. Sprinkle, C. Berger, C. N. Lau, W. A. deHeer, E. H. Conrad and R. C. Haddon, *Nano Lett.*, 2010, **10**, 4061–4066.

